



UNIVERSITEIT VAN PRETORIA
UNIVERSITY OF PRETORIA
YUNIBESITHI YA PRETORIA

**The geology of the Blouberg Formation, Waterberg and Soutpansberg Groups in
the area of Blouberg mountain, Northern Province, South Africa**

by

ADAM JOHN BUMBY

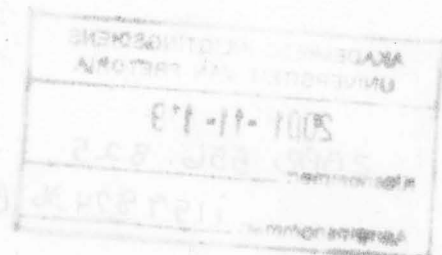
Submitted in partial fulfillment of the requirements for the degree

DOCTOR OF PHILOSOPHY

**in the Faculty of Science
University of Pretoria**

PRETORIA

November 2000





**THIS THESIS REPRESENTS THE ORIGINAL WORK
OF THE AUTHOR, EXCEPT WHERE SPECIFIC
ACKNOWLEDGEMENT IS MADE
TO THE WORK OF OTHERS**

November 2000

ABSTRACT.

The geology of the Blouberg mountain area, Northern Province, South Africa is characterised by a number of successor basins developed over a region which is underlain by a cratonic suture (the Palala Shear Zone). The suture was formed during the Limpopo Orogeny, due to oblique convergence of the Kaapvaal Craton and the Central Zone of the Limpopo Mobile Belt at either 2.65Ga or 2.0Ga. Post-collisional brittle reactivation along the Palala Shear Zone in the Blouberg study area is accommodated on the parallel Melinda Fault.

The earliest basin developed in this area was that of the Blouberg Formation, which is preserved in an area restricted to the eastwards extension of the Palala Shear Zone. The Blouberg Formation can be divided into Lower and Upper Members. The widespread Lower Member is thought to have been deposited in a pull-apart basin, is characterised by braided fluvial sheetflood deposits, and is generally steeply-dipping or overturned, reflecting a subsequent southwards-vergent basin inversion. The Upper Member contrasts with the Lower Member in that it is preserved only rarely, is generally flat-lying, and is composed of conglomerates with sub-angular cobbles of foliated basement rocks with rare granulestone beds, reflecting deposition in debris flows and braided rivers respectively. The tectonic event responsible for the southwards-vergent basin inversion of the Lower Member probably also uplifted proximal basement sources to the north and east, leading to deposition of the Upper Member in localised basins close to the southern strand of the Melinda Fault scarp.

The syn-tectonic deposition of the Blouberg Formation was followed by a period of relative tectonic quiescence, and deposition of the Waterberg Group. The fluvial Setlaole Formation was succeeded by the predominantly aeolian Makgabeng Formation. Strata of these two formations are not preserved north of the Melinda Fault, probably due to the syn-Blouberg tectonic activity, which had led to development of high topography in this area. This palaeohigh gradually denuded throughout Waterberg sedimentation.

Ultimately, the Mogalakwena Formation, the youngest of the Waterberg units in the study area, overlapped northwards over these denuding highlands.

After the end of Mogalakwena deposition, renewed tectonic activity led to approximately north-south orientated extension. Syn-Blouberg northwards-dipping reverse faults along the southern strand of the Melinda Fault were locally reactivated as normal faults, resulting in a half-graben type environment. A depository was created above the hanging wall, which filled with the strata of the Soutpansberg Group; initially volcanics of the Sibasa Formation erupted, followed by the clastic deposition of the Wyllies Poort Formation.

Late-stage reactivation along the Palala Shear Zone is represented by the northern strand of the Melinda Fault, which is generally a dextral strike-slip fault, with up to 17km of total displacement.

SAMEVATTING.

Die geologie van die Blouberg omgewing in die Noordelike Provinsie van Suid-Afrika word gekenmerk deur die teenwoordigheid van 'n aantal opeenvolgende sedimentêre komme wat ontwikkel is oor 'n kratoniese sutuursone (die Palala skuifskeursone). Die sutuur het gevorm tydens die Limpopo Orogenese (2.65 of 2.0 Ga) en was die gevolg van skuins konvergensie van die Kaapvaalkraton en die Sentralesone van die Limpopo Mobiele Gordel. Bros heraktivering van die Palala skuifskeursone in die Blouberg studiegebied, na die botsing, het plaasgevind op Melindaverskuiwing.

Die eerste kom wat ontwikkel het in die studiegebied, is gevul deur die Blouberg Formasie, wat gepreserveer is in 'n gebied wat beperk is tot die oostelike verlenging van die Palala skuifskeursone. Die Blouberg Formasie kan onderverdeel word in 'n Onderste en Boonste Lid. Die wydverspreide Onderste Lid is klaarblyklik in 'n ooptrekking afgesit en word gekenmerk deur gevlegde fluviale plaatvloed afsettings wat algemeen steilhellend tot oorgeplooi is deur 'n jonger, suidwaarts gerigte kominversie. Die Boonste Lid verskil van die Onderste Lid deur dat dit swak gepreserveer is, oor die algemeen horisontaal gelaagd is, en bestaan uit konglomeraat met sub-hoekige rolstene van gefolieerde vloergesteentes en korrelsteenlae. Laasgenoemde sedimente dui respektiewelik op puinvloei en gevlegde riviere. Die tektoniese gebeurtenis verantwoordelik vir die suidwaarts gerigte kominversie van die Onderste Lid het ook proksimale vloergesteente bronne in die noorde en ooste opgehef. Dit het gelei tot die afsetting van die Boonste Lid in gelokaliseerde komme naby die suidelike vertakking van die Melindaverskuiwingsesekarp.

Die sintektoniese afsetting van die Blouberg Formasie is gevolg deur 'n relatief tektonies-statische tydperk waartydens die Waterbergkom gevul is. Die fluviale Setlaole Formasie is gevolg deur die eoliese Makgabeng Formasie. Sedimente van hierdie twee formasies is nie noord van die Melindaverskuiwing gepreserveer nie, waarskynlik as gevolg van die sin-Blouberg tektoniese aktiwiteit wat hoë topografie in die gebied tot gevolg gehad het. Hierdie paleohoog is geleidelik tydens Waterberg sedimentasie vernietig. Uiteindelik het



die Mogalakwena Formasie, die jongste van die Waterberg eenhede in die studiegebied, hierdie hooglande na die noorde oordek.

Na die einde van Mogalakwena afsetting het hernude tektoniese aktiwiteit gelei tot noord-suid korsverlenging. Sin-Blouberg noordwaartshellende oorskuiwings, langs die suidelike vertakking van die Melindaverskuiwing, is plaaslik geheraktiveer as afskuiwings wat 'n halwe-graben omgewing tot gevolg gehad het. 'n Afsettingskom is gevorm op die dakkant en is gevul deur gesteentes van die Soutpansberg Groep, bestaande uit vulkaniese gesteentes van die Sibasa Formasie gevolg deur klastiese gesteentes van die Wyllies Poort Formasie.

Laat-stadium heraktivering van die Palala skuifskeursone word deur die noordelike vertakking van die Melindaverskuiwing verteenwoordig en aanduidings is dat daar sowat 17 km regs-laterale strekkingsglijpverplasing is.



TABLE OF CONTENTS.

	Page
CHAPTER 1: INTRODUCTION	1
1.1 Location of the study area	1
1.2 Regional Geology	1
1.2.1: The Limpopo Mobile Belt	2
1.2.2: The Blouberg Formation	4
1.2.3: The Waterberg Group	5
1.2.4: The Soutpansberg Group	9
1.2.5: The Melinda Fault Zone	10
1.3: Previous work in the Blouberg area	11
1.3.1: Summary of the work of Jansen (1976)	11
1.3.1.1: Stratigraphic units examined by Jansen (1976)	11
1.3.1.2: Stratigraphic relationships proposed by Jansen (1976)	13
1.3.1.3: Mode of deposition proposed by Jansen (1976)	15
1.3.1.4: Basin evolution of the Blouberg area proposed by Jansen (1976)	16
1.3.1.5: Conclusions (Jansen, 1976)	17
1.3.2: The work of Meinster (1977)	18
1.3.3: The work of Brandl (1991)	21
1.4: Relevant previous work in surrounding areas	21
1.4.1: Previous work on the Limpopo Mobile Belt	21
1.4.2: Previous work on the Waterberg Group	23
1.4.2.1: Early work on the Waterberg Group (1872-1982)	23
1.4.2.2: Recent work on the Waterberg Group (1977-present)	26
1.4.3: Previous work on the Soutpansberg Group	29
1.5: Aims of the study	32
1.6: Methodology	33
1.6.1: Field work	33
1.6.2: Photogeology	35
1.6.3: Geological maps and cross-sections	35
1.6.4: Calculations of palaeohydrological parameters	35
1.6.4.1: Palaeohydrological parameters that can be calculated from clast-filled channels	36
1.6.4.2: Palaeohydrological parameters that can be calculated from cross-bed set thickness	37
1.6.5: Laboratory methods	39
CHAPTER 2: PRE-BLOUBERG, WATERBERG AND SOUTPANSBERG ROCKS	57
CHAPTER 3: THE BLOUBERG FORMATION	73
3.1: Introduction	73



3.2: Description of type section of Blouberg Formation	74
3.2.1: Architectural Elements	74
3.2.2: Facies and Facies Associations	75
3.3: Blouberg Formation in the area of Blouberg mountain	78
3.4: Palaeocurrent analysis	83
3.5: Palaeohydraulics	84
CHAPTER 4: THE WATERBERG GROUP	120
4.1: Introduction	120
4.2: Setlaole Formation	120
4.3: Makgabeng Formation	122
4.3.1: Bounding surfaces in aeolian sediments	123
4.3.2: Bounding surfaces present in the Makgabeng Formation	126
4.3.3: Facies associations present in the Makgabeng Formation	127
4.3.3.1: Large-scale trough and planar cross-bedded sandstone facies association	127
4.3.3.2: Horizontally bedded and rippled mudstone and sandstone facies association	129
4.3.3.3: Rippled and cross-bedded sandstone facies association	131
4.3.3.4: Massive sandstone facies association	132
4.3.3.5: Pebbly sandstone facies association	133
4.4: Mogalakwena Formation	135
4.4.1: Mogalakwena strata south of the southern strand of the Melinda Fault	135
4.4.1.1: Eastern part of the study area	135
4.4.1.2: Western part of the study area	140
4.4.2: Mogalakwena strata north of the southern strand of the Melinda Fault	142
CHAPTER 5: THE SOUTPANSBERG GROUP	192
5.1: The Sibasa Formation	192
5.2: The Wyllies Poort Formation	193
CHAPTER 6: INTRUSIVE ROCKS	210
CHAPTER 7: MAP RELATIONSHIPS AND STRUCTURAL GEOLOGY	217
7.1: Structures present within the basement gneiss	217
7.2: Structures present within the Blouberg Formation	218
7.3: Structures present within the Setlaole Formation	220
7.4: Structures present within the Makgabeng Formation	220
7.5: Structures present within the Mogalakwena Formation	221
7.6: Structures present within the Sibasa and Wyllies Poort Formations	222
7.7: Relationships present between stratigraphic units in the study area	224
7.8: Relationships formed by intrusive rocks	227



CHAPTER 8: GEOLOGICAL HISTORY	252
8.1: Tectonic setting	252
8.1.1: Tectonic interpretation of basement rocks	252
8.1.2: Tectonic interpretation of the Blouberg Formation	253
8.1.3: Tectonic interpretation of the Waterberg Group (Setlaole, Makgabeng and Mogalakwena formations)	255
8.1.4: Tectonic interpretation of the Soutpansberg Group	257
8.1.5: Conclusions regarding the age relationships and tectonic setting in the study area	259
8.2: Depositional palaeoenvironments	260
8.2.1: Depositional setting of the Blouberg Formation	260
8.2.2: Depositional setting of the Setlaole Formation	264
8.2.3: Depositional setting of the Makgabeng Formation	264
8.2.4: Depositional setting of the Mogalakwena Formation	269
8.2.5: Depositional setting of the Wyllies Poort Formation	271
8.3: Provisional basin evolution model for the study area	273
CHAPTER 9: ECONOMIC POTENTIAL	289
CHAPTER 10: CONCLUSIONS	290
ACKNOWLEDGEMENTS	294
REFERENCES	295
APPENDIX 1	Geological map of the study area
APPENDIX 2	Data from pebble survey in the Mogalakwena Conglomerates
APPENDIX 3	Cross-sections through the Blouberg mountain area, constructed from geological map



LIST OF FIGURES.

1.1: Geographical location of the study area	41
1.2: Map showing geographical features of the study area	42
1.3: Simplified geological map and cross-section showing features of the Limpopo Mobile Belt (after Kröner <i>et al.</i> , 1999 and Roering <i>et al.</i> , 1992)	43
1.4: Map showing the distribution of the lithostratigraphic units in the Blouberg Formation (after Jansen, 1982)	44
1.5: The distribution of the Waterberg Group (after Callaghan <i>et al.</i> , 1991)	45
1.6: Map showing the distribution of the lithostratigraphic units in the main Warmbaths basin of the Waterberg Group (after Callaghan <i>et al.</i> , 1991)	46
1.7: Map showing the distribution of the lithostratigraphic units in the Soutpansberg Group (after Barker <i>et al.</i> , in press)	47
2.1: Quarto-feldspathic banded gneiss with dark amphibolite lenses, exhibiting vertically-dipping, 080°-striking foliation. Sub-euhedral feldspar porphyroclasts show stair-stepping and suggest sinistral movement along the foliation plane	61
2.2: Photomicrograph of thin section of basement gneiss	61
2.3: Photomicrograph of a thin section from an amphibolite lens in banded gneiss	62
2.4: Stereographic projection showing the poles of generally vertically-dipping foliation planes recorded in basement gneiss	63
2.5: Banded gneiss showing 080°-striking foliation, boudinage structures and pegmatite veins.	62
2.6: 'S'-shaped folds in foliated gneiss; sinistral strike-slip movement	64
2.7: Vertically-plunging 'S'-shaped folds in basement gneiss	64
2.8: Stereographic projection showing poles of foliation planes in basement gneiss	65
2.9: Primary and secondary foliation planes in basement gneiss	66
2.10: Partial melting in basement gneiss	66
2.11: Map showing the strike of foliation planes at My Darling	67
2.12: Primary and Secondary foliation in basement gneiss at My Darling	68
2.13: Rose diagrams showing the strike of primary and secondary foliation planes in banded gneiss	69
2.14: Friable crush breccia from the southern strand of the Melinda Fault	68
2.15: Crush breccia intruded by thin quartz-filled veins on the southern strand of the Melinda Fault	70
2.16: Photomicrograph of quartz veins intruding quartzo-feldspathic gneiss	70
2.17: Stereographic projection showing poles to planes defined by quartz veins along the southern strand of the Melinda Fault	71
2.18: Hydrothermally altered rock from the contact between the southern strand of the Melinda Fault and the Blouberg Formation	72
3.1: Stratigraphic section of the Blouberg Formation in the Kranskop area	86-91
3.2: Small trough cross-bedded sets in facies association 1 of the Blouberg Formation	92
3.3: Pebbly granulestone-filled channel form in facies association 1 of the	



Blouberg Formation	92
3.4: Photomicrograph of coarse sandstone from facies association 1	93
3.5: Detail of pebbly granulestone, showing arkosic nature of sediment	93
3.6: Coarse sandstone and granulestone-filled channel forms in facies association 2	94
3.7: Small (<10cm) sets of trough cross-bedded sandstone in facies association 2	94
3.8: Soft sediment deformation in facies association 2	95
3.9: Photomicrograph of coarse sandstone of facies association 2	95
3.10: Conglomerate from facies association 3 of the Blouberg Formation	96
3.11: Detail of conglomerate from facies association 3	96
3.12: Fining-upwards cyclicity in facies association 3	97
3.13: Clast-supported conglomerate fine upwards into a sandstone-filled channel form	97
3.14: Photomicrograph of interclast material from conglomerate in facies association 3	98
3.15: Conglomerate and sandstone sheets of facies association 4	98
3.16: Channel-fill in the Blouberg Formation in the Blouberg mountain area	99
3.17: Detail of coarse feldspathic granulestone	99
3.18: Cobbles of foliated gneiss in a matrix of granulestone in the Blouberg Formation	100
3.19: Trough and planar cross-bedded sandstone and granulestone with quartz cobbles	100
3.20: Thick cosets of cross-bedded sandstone and granulestone	101
3.21: Sets of cross-bedded sandstone and granulestone with quartz cobbles on foresets	101
3.22: Photomicrograph of sandstone from Blouberg Formation in Blouberg mountain area	102
3.23: Steeply-dipping trough cross-bedded sandstone in the Blouberg Formation	102
3.24: Muddy sandstone in the Blouberg Formation with fault propagation fold	103
3.25: Weakly foliated cobbles of basement gneiss in the Blouberg Formation	103
3.26: Stratigraphic section of the Blouberg Formation in the Dantzig area	104
3.27: Cobbles of feldspathic gneiss in the Blouberg Formation	105
3.28: Large-scale trough cross-bedding in the Blouberg Formation	105
3.29: Vertically-dipping planar cross-bedded granulestone	106
3.30: Laminated muddy sandstone in the Blouberg Formation	106
3.31: Steeply-dipping strata of the Blouberg Formation, with sand-filled channel form	107
3.32: Rose diagram showing palaeocurrent directions for the Kranskop strata of the Blouberg Formation	108
3.33: Rose diagram showing palaeocurrent directions for the Blouberg Formation in the Blouberg mountain area	109
3.34: Rose diagram showing palaeocurrent directions for the Upper Member of the Blouberg Formation in the Blouberg mountain area	110
3.35: Map showing the location of outcrops of the Blouberg Formation, variability in palaeocurrent directions and the location of sites from which palaeohydraulic parameters were recorded	111



3.36: Histograms showing variability in palaeohydrological parameters calculated from clast sizes within channels	112
3.37: Histograms showing variability in palaeohydrological parameters across the Blouberg basin	113
3.38: Histograms showing variability in palaeohydrological parameters across the Blouberg basin	114
4.1: Trough cross-bedded coarse sandstone and granulestone in the Setlaole Formation	146
4.2: Detail of foliated clasts in the Setlaole Formation	146
4.3: Rose diagram to show palaeocurrent directions in the Setlaole Formation	147
4.4: Nonconformity between basement and Setlaole Formation	148
4.5: Trough cross-bedded sets coarse/very coarse grained sandstone in the Setlaole Formation	148
4.6: Pale-coloured pebbly granulestone facies in the Setlaole Formation	149
4.7: Rose diagram showing showing palaeocurrent directions from the type locality	150
4.8: Photomicrograph of the Setlaole Formation	149
4.9: Pale-coloured pebbly granulestone from near My Darling	151
4.10: Pale coloured trough cross-bedded conglomerate and granulestone	151
4.11: Photomicrograph from a sandstone clast from a conglomerate layer in the Setlaole Formation	152
4.12: Borehole log from Vleypan 411	153-156
4.13: Second-order surface developed between sets of large-scale trough cross-bedding in the Makgabeng Formation	152
4.14a: Third-order (reactivation) surfaces in the Makgabeng Formation	157
4.14b: Sketch illustrating climbing bedforms and horizontal super-surfaces	157
4.15: Super-surface developed between the Makgabeng Formation and the Mogalakwena Formation	158
4.16: Photomicrograph showing inverse-grading in Makgabeng Formation sandstone	158
4.17: Asymmetric ripplemarks in the Makgabeng Formation	159
4.18: Steeply-inclined cross-beds in the Makgabeng Formation	159
4.19: Wedge-shaped strata tapering in a down-dip direction	160
4.20: Map showing relationships between sets of large-scale trough cross-beds	161
4.21: Horizontally-bedded and rippled mudrocks with interbedded sandstone	160
4.22: Current ripples and desiccation cracks in mudrock in the Makgabeng Formation	162
4.23: Muddy roll-up structures in the Makgabeng Formation	162
4.24: Muddy roll-up structures in the Makgabeng Formation	163
4.25: Evaporite casts (possibly gypsum) in the Makgabeng Formation	163
4.26: Massive sandstone facies in the Makgabeng Formation	164
4.27: Lens-shaped massive sandstone beds onlapping onto third-order surfaces	164
4.28: Channelised massive sandstone	165
4.29: Photograph illustrating erosive nature of massive sandstone	165
4.30: Soft sediment deformation, with laminations having slumped down	



foresets	166
4.31: Channelised contact between inversely-graded strata and strata of the pebbly sandstone facies association	166
4.32: Planar laminated sandstone with quartz pebbles	167
4.33: Small sets of planar cross-bedded sandstone with quartz-pebbles on foresets	167
4.34: Parting lineation on planar bedding surfaces in pebbly sandstone facies association	168
4.35: Rose diagram showing palaeocurrent directions in the pebbly sandstone facies association	169
4.36: Inversely-graded sandstones are overlain and channelised by strata of the pebbly sandstone facies association	168
4.37: Interbedded conglomerate and sandstone sheet-like elements in the Mogalakwena Formation	170
4.38: Interbedded sandstone and conglomerate sheets	170
4.39: Large-scale conglomerate-filled channel forms within sheet-like architectural elements in the Mogalakwena Formation	171
4.40: Rare imbricated conglomerates and cross-bedded sandstone sheets in the Mogalakwena Formation	171
4.41: Well-rounded, massively bedded conglomerate	172
4.42: Cobbles of quartz, quartzite and B.I.F. in the Mogalakwena Formation	172
4.43: Plan view of trough cross-bedded sandy sheets	173
4.44: Photomicrograph of sandstone from sandy sheets	173
4.45: Photomicrograph of matrix from Mogalakwena conglomerate	174
4.46: Map showing outcrops of the Mogalakwena Formation and location of recording sites for pebble survey	175
4.47: Graph showing the variance in % of clasts with stratigraphic height	176
4.48: Graph showing the variance in % of clasts from N to S	179
4.49: Graph showing the variance in clast size with stratigraphic height	177
4.50: Graph showing the variance in average clast size from N to S	179
4.51: Graph showing the variance of 'index of coarseness' with stratigraphic height	178
4.52: Graph showing the variance in 'index of coarseness' from N to S	179
4.53: Graph showing the variance in total percentages for each clast composition with stratigraphic height	180
4.54: Graph showing the N-S variance in quartz, quartzite and B.I.F. cobbles	181
4.55: Rose diagram to show palaeocurrent directions in the Mogalakwena Formation south of the southern strand of the Melinda Fault in the eastern part of the study area	182
4.56: Sheet-like architectural elements in the western outcrops of the Mogalakwena Formation	183
4.57: Conglomerate-filled channel in the western outcrops of the Mogalakwena Formation	183
4.58: Small (<10cm) sets of trough cross-bedded sandstone with heavy mineral drapes on foresets in the western outcrops of the Mogalakwena Formation	184
4.59: Small-scale trough cross-beds in sandstone of the Sandriviersberg Formation	184

4.60: Photomicrograph of sandstone from sandy sheets in the western part of the study area	185
4.61: Rose diagram showing palaeocurrent directions recorded from western (distal) parts of the study area	186
4.62: Sheet-like architectural elements of coarse sandstone and granulestone in Mogalakwena strata north of the southern strand of the Melinda Fault	185
4.63: Thin basal conglomerates of the Mogalakwena Formation north of the southern strand of the Melinda Fault	187
4.64: Detail of basal conglomerate in the Mogalakwena Formation north of the southern strand of the Melinda Fault	187
4.65: Trough cross-bedded sandstone and granulestone in the Mogalakwena Formation north of the southern strand of the Melinda Fault	188
4.66: Small scale (<10cm) sets of trough cross-bedded sandstone with heavy mineral drapes on foresets, from north of the southern strand of the Melinda Fault	188
4.67: Small scale (<10cm) sets of trough cross-bedded sandstone with heavy mineral drapes on foresets, from north of the southern strand of the Melinda Fault	189
4.68: Photomicrograph of the Mogalakwena Formation in the northern foothills of Blouberg mountain	189
4.69: Photomicrograph of the Mogalakwena Formation in the southern foothills of Blouberg mountain, just north of the southern strand of the Melinda Fault	190
4.70: Rose diagram showing palaeocurrent directions from the Mogalakwena Formation north of the southern strand of the Melinda Fault	191
5.1: Amgdaloidal basalt of the Sibasa Formation	197
5.2: Ropey lava texture in basalt of the Sibasa Formation	197
5.3: T.A.S. diagram showing classification and nomenclature of Sibasa basalts	198
5.4: Photomicrograph of Sibasa basalt	199
5.5: Spidergram showing values of incompatible trace elements in the Sibasa Formation	200
5.6: Quartz pebble layer in the Wyllies Poort Formation	199
5.7: Oblique aerial photograph showing horizontally inclined sheet-like architectural elements, with an absence of preserved channel forms	201
5.8: Map showing the location of a stratigraphic section recorded through the Wyllies Poort Formation	202
5.9: Small trough cross-bedded sets in the lower Wyllies Poort Formation, with soft sedimentary deformation	201
5.10: Large symmetric ripples in the mid-Wyllies Poort Formation	203
5.11: Linguoid ripples in the upper strata of the Wyllies Poort Formation	203
5.12: Asymmetric ripplemarks in the Wyllies Poort Formation	204
5.13: Large scale trough cross-beds, interbedded with low angled planar cross-beds in the mid- Wyllies Poort Formation	204
5.14: Plan section of sand volcano in the mid-Wyllies Poort Formation	205
5.15: Photomicrograph of Wyllies Poort quartzite	205
5.16: Photomicrograph of Wyllies Poort sandstone	206
5.17: Photomicrograph of a sandstone pebble from a Wyllies Poort pebble layer	206
5.18: Photomicrograph of coarse sandstone from the Mogalakwena Formation	207

5.19: Rose diagrams showing palaeocurrent directions recorded in different facies of the Wyllies Poort Formation	208
6.1: Gently-dipping dyke cutting the Mogalakwena Formation	212
6.2: Rose diagram showing the orientation of dykes cutting the Waterberg Group	213
6.3: E.N.E.-striking, vertically-dipping dyke cutting the Blouberg Formation	212
6.4: TAS diagram showing nomenclature for dykes (after Wilson, 1989)	214
6.5: Spidergram showing values of incompatible trace elements in dykes	215
7.1: Crush-breccia on the southern strand of the Melinda Fault	228
7.2: Detail of crush breccia	228
7.3: Crush breccia with quartz veins	229
7.4: Low-angled foliation developed on thrust fault	229
7.5: Horizontal slickensided surface in basement gneiss	230
7.6: Stereographic projection showing poles of low-angled thrust fault planes cutting the basement gneiss	231
7.7: Stereographic projection showing poles to bedding planes in the Blouberg Formation	232
7.8: Folding developed in the Blouberg Formation at Varedig	230
7.9: Stereographic projection showing poles to bedding planes in Blouberg strata at Varedig	233
7.10a: Steeply-dipping reverse fault cutting the Blouberg Formation, but not the overlying Mogalakwena Formation	234
7.10b: Explanation of observed structures by the presence of large-scale, southward-vergent thrust fault, displacing the Blouberg Formation	235
7.11: Stereographic projection showing the orientation of slickenside lineations in the Blouberg Formation	235
7.12: Slickensides developed in the Blouberg Formation	234
7.13: Jointing in the lower Wyllies Poort Formation	236
7.14: Jointing developed in ripplemarked upper strata of the Wyllies Poort Formation	236
7.15: Fault developed in the lower strata of the Wyllies Poort Formation, showing evidence for dextral strike-slip movement	237
7.16: Sketch showing relationship between bedding-parallel thrust, folded joint planes and slickenside lineations	238
7.17: Stereographic projection showing poles to bedding planes in the Wyllies Poort Formation in the vicinity of the northern strand of the Melinda Fault	239
7.18: Quartz-filled veins intruding the Wyllies Poort Formation	237
7.19: Quartz-filled veins intruding a brittle fault in the Wyllies Poort Formation	240
7.20: Sinistral dilatational vein in the Wyllies Poort Formation	240
7.21: Wide quartz-filled vein in the Wyllies Poort Formation	241
7.22: Small hill underlain by white quartzite on the northern strand of the Melinda Fault	241
7.23: Fault breccia in the Wyllies Poort Formation	242
7.24: Fault plane with preserved fault breccia	242
7.25: Fault breccia with weak S-C fabric	243



7.26: Rose diagram showing the strike of joints in the Wyllies Poort Formation	244
7.27: Rose diagram showing the strike of veins cutting the Wyllies Poort Formation	245
7.28: Stereographic projection of poles to fault planes in the Wyllies Poort Formation	246
7.29: Stereographic projection showing the orientation of slickenside lineations in the Wyllies Poort Formation	247
7.30: Pronounced angular unconformity between the Blouberg and Mogalakwena formations	243
7.31: Pronounced angular unconformity between the Blouberg and Mogalakwena formations	248
7.32: Pronounced angular unconformity between the Blouberg and Mogalakwena formations	248
7.33: Disconformity between the Makgabeng and Mogalakwena formations	249
7.34: Disconformity between the Makgabeng and Mogalakwena formations, showing joint planes	249
7.35: Joint plane in the Makgabeng Formation is exploited as a channel during the onset of Mogalakwena deposition	250
7.36: Reduction spot developed in upper Makgabeng strata, but not in lower Mogalakwena strata	250
7.37: Gentle angular unconformity developed between the Mogalakwena and the Wyllies Poort formations	251
7.38: Detail of the gentle angular unconformity developed between the Mogalakwena and Wyllies Poort formations	251
8.1: Spidergram to compare incompatible trace elements for dykes and Sibasa basalts	279
8.2: Variation diagram between incompatible elements Zr and Y, for dykes and Sibasa basalts, to show a common parental magma	280
8.3: Strain ellipse which accounts for structures recorded in the Wyllies Poort Formation adjacent to the northern strand of the Melinda Fault	281
8.4: Map showing approximate line of idealised cross-section (Figure 8.5)	282
8.5: Idealised cross-section through Blouberg mountain, illustrating structural relationships	283
8.6: Block diagrams illustrating the proposed model for tectonic and sedimentary evolution of the Blouberg area	284-286



LIST OF TABLES

1.1: Stratigraphic subdivision of the Blouberg Formation (after S.A.C.S., 1980)	48
1.2: Stratigraphic subdivision of the Waterberg Group (after Callaghan <i>et al.</i> , 1991)	49
1.3: Stratigraphic subdivision of the Soutpansberg Group (after S.A.C.S., 1980)	50
1.4: Summary of the work of the Limpopo Working Group, 1977-1982	51
1.5: Summary of work on the Limpopo Mobile Belt in the Geology Society of South Africa special publication (Van Biljon and Legg, 1983)	52
1.6: Summary of recent work on the Limpopo Mobile Belt (1982-1999)	53
1.7: Summary of early work on the Waterberg Group, 1872-1965)	54
1.8: Summary of work on the Waterberg Group undertaken by the Geological Survey of South Africa, 1963-1982	55
1.9: Summary of early work on the Soutapnsberg Group, 1908-1955	56
3.1: Architectural elements and facies grouping for fluvial deposits	115
3.2: Palaeohydrological parameters calculated from clast size and channel dimensions in the Blouberg Formation	116
3.3a,b,c: Palaeohydrological parameters calculated from set heights in the Blouberg Formation	117-119
5.1: X.R.F. and I.C.P.M.S. results major and trace element abundances in samples of Sibasa Foramtion basalt	209
6.1: X.R.F. and I.C.P.M.S. results for major and trace element abundances in samples of dykes	216
8.1: Proposed new stratigraphic subdivision of the study area, comparing with the existing stratigraphic subdivision	287
8.2a,b: Interpretation of facies assemblages and architectural elements (after Miall, 1992)	288